A&A 433, 635–639 (2005)
DOI: 10.1051/0004-6361:20042314

Astronomy & Astrophysics

A serendipitous *XMM-Newton* observation of the intermediate polar WX Pyx⋆

E. M. Schlegel

High Energy Astrophysics Division, Smithsonian Astrophysical Observatory, Cambridge, MA 02138, USA
e-mail: eschlegel@cfa.harvard.edu

Received 4 November 2004 / Accepted 8 December 2004

Abstract. We briefly describe a serendipitous observation of the little-studied intermediate polar WX Pyx using *XMM-Newton*. The X-ray spin period is 1557.3 s, confirming the optical period published in 1996. An orbital period of ∼5.54 h is inferred from the separation of the spin-orbit sidelobe components. The soft and hard band spin-folded light curves are roughly sinusoidal in shape. The best-fit spectrum is consistent with a bremsstrahlung temperature of ∼18 keV. An upper limit of ∼300 eV is assigned to the presence of Fe line emission. WX Pyx lies near TX and TV Col in the $P_{\rm spin} - P_{\rm orb}$ plane.

Key words. X-rays: individuals: WX Pyx – X-rays: binaries – stars: novae, cataclysmic variables

1. Introduction

WX Pyx, originally designated 1E 0830.9-2238, was uncovered in a survey of the Galactic plane using *Einstein* (Hertz & Grindlay 1984) and described in more detail by Hertz et al. (1990). Those authors identified the probable counterpart by searching for objects with the highest UV excess. An optical spectrum of 1E 0830 showed emission lines typical of a cataclysmic variable (=CV), including Hβ, Hγ, and He II. The large value of the He II/Hβ emission ratio suggested a magnetic CV although that ratio is not a unique indicator (Szkody 1990). 1E 0830 acquired its new name on the 71st Namelist of Variable Stars (Kazarovets et al. 1993).

Remarkably, there has been no detailed follow-up of this CV in the X-ray band and little in any waveband. O'Donoghue et al. (1996) supplied the only detailed study to date using optical photometry. They uncovered a stable period of 26 min they assumed was the spin period, indications of an orbital period of very roughly 6 h, and raised the distinct possibility that the counterpart was an intermediate polar (IP). It was included in three surveys for radio emission (Pavelin et al. 1994; Beasley et al. 1994; Wendker 1995) and a survey of infrared emission from the 2MASS survey (Hoard et al. 2002). As with most CVs, WX Pyx was not detected in the radio but was seen in the IR. Buckley (2000) included it on a list of "to be observed" objects in a summary of the power spectra of IPs. To date, the spin and orbital periods remain unconfirmed.

Intermediate polars (=IP) are a subclass of magnetic CVs in which the magnetic moment is insufficiently strong to dominate the dynamics of the accretion flow completely. As a result, the spin period of the accreting white dwarf is not magnetically locked to the orbital period as in the polars (e.g., Warner 1995). The defining characteristic of an IP is the presence of a strong pulse in the X-ray band marking the spin of the white dwarf. IPs generally show hard spectra with a bremsstrahlung kT in the 10–30 keV range and strong Fe K line emission.

We describe a serendipitous observation of WX Pyx by *XMM-Newton*.

2. Observation

WX Pyx was observed for ∼45 ks during a pointed observation of NGC 2613, PI = T. Chaves, on 2003 Apr. 23 (obsid 0149160101). WX Pyx lies ∼10.5′ offaxis to the northwest. The large off-axis angle ensures that only data from the EPIC-PN and -MOS detectors includes WX Pyx; the source lies outside the fields-of-view of the Optical Monitor and Reflection Gratings. The April observation was hammered by soft X-ray flares; at best, ∼20% of the observation may be salvaged. A second observation of NGC 2613 occurred on 2003 May 20 for 29 299 s (obsid 0149160201). This observation contains considerably fewer flares, losing <30% of the data to flaring activity. For both observations, the EPIC-PN used the thin filter. Table 1 summarizes the available data. Figure 1 shows the filtered light curves for the May EPIC-PN data in the soft (0.5–2 keV) and hard (2–10 keV) bands as well as the hardness ratio (hard/soft).

3. Light curve and power spectrum

From an extracted light curve, times of flaring activity were identified and subsequently filtered from the data sets. Even in perfect data sets, the count rate in the MOS detectors is perhaps

⋆ Research supported by contract number NAS8-39073 to SAO.

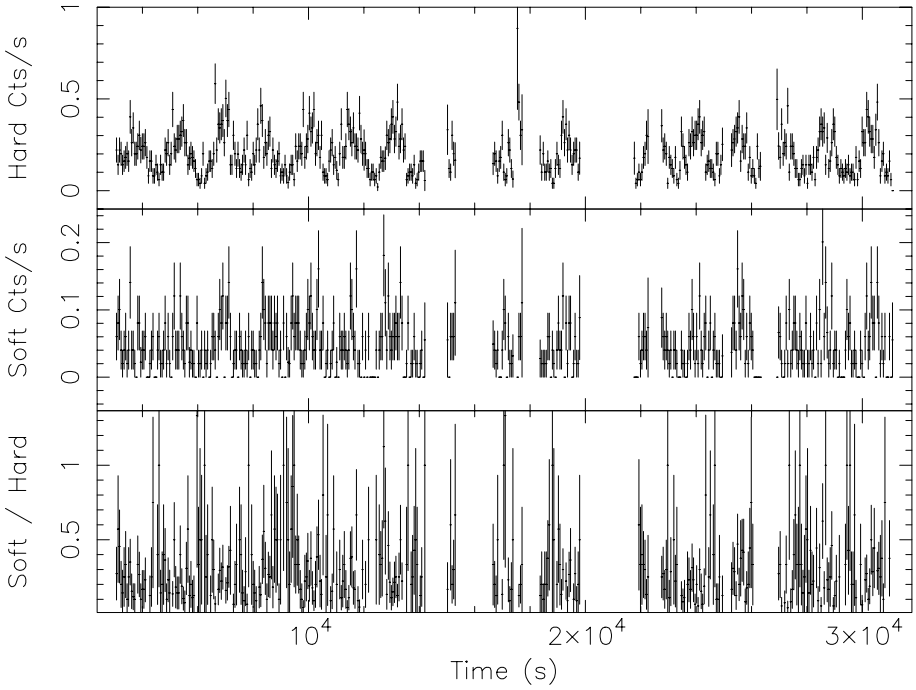

Fig. 1. Soft and hard light curves and hardness ratios of WX Pyx for May 2003 PN data.

Table 1. *XMM-Newton* observations of WX Pyx.

No.	Obsid	Date	Original expT	Filtered expT	Source count rate	Detectors used
1	0149160101	2003 Apr. 23	45255	9478	0.04	PN only
2	0149160201	2003 May 20	29919	25 189	0.24	PN
	...	...	...	27 250	0.07	MOS-1
	...	...	...	27 299	0.05	MOS-2

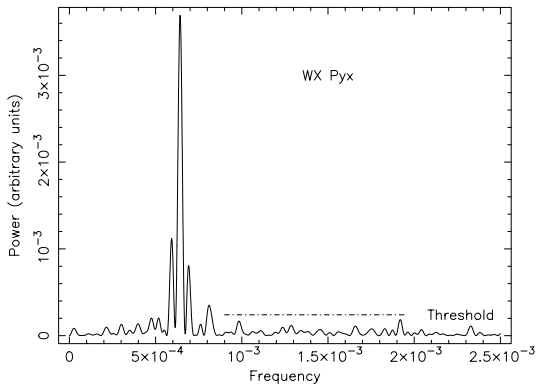

Fig. 2. Power spectrum for May EPIC-PN observation of WX Pyx. The peaks near 6.4×10^{-4} are identified as the $\omega - \Omega$, ω, and $\omega + \Omega$ frequency components, respectively. The dashed line is the approximate 3σ detection threshold.

a third of the EPIC-PN detector. Given the flaring in the April observation, only the first 9 ks could be used; combining the lower count rate for the MOS detectors and the short data span, we used only the EPIC-pn data. For the May observation, data from the PN and MOS detectors were used, suitably filtered to eliminate the times of flares (Table 1).

Applying an FFT to the full-band light curve yielded the power spectrum shown in Fig. 2. Three Gaussians plus a constant were fit to the data to determine the centroids of the power spectrum components. The peak is identified as the spin period ω of the IP; the two lower peaks are the sidelobes of $\omega - \Omega$ and $\omega + \Omega$. The fitted spin frequency is $6.42146 \pm 0.00075 \times 10^{-4}\,\mathrm{s}^{-1}$, corresponding to a spin period of 1557.3 ± 0.3 s where the error is conservatively adopted as the 90% confidence range on the center of the Gaussian.

From the $\omega - \Omega$ and $\omega + \Omega$ values, the orbital frequency is $\sim 5.0167 \times 10^{-5}$ s^{-1} corresponding to an orbital period of $\sim 19\,933$ s $\sim$ 5.54 h. If we determine the spin frequency from the $\omega - \Omega$ and $\omega + \Omega$ values, that value differs from the fitted spin frequency by ~0.06%. Applying that difference to the orbital period implies an estimated uncertainty in orbital period of ~15–20 s. That no power appears in the power spectrum at the orbital period is not surprising given that the filtered observation is at best ~1.5 times the length of the orbital period. The counts in the soft and hard bands for each P_{spin} interval were summed and a sinusoid fit to the resulting light curve to detect or place a limit on orbital modulation. The estimates of the orbital modulation are 0.006 ± 0.003 for the soft band and 0.014 ± 0.008 for the hard band where the errors are 90% for

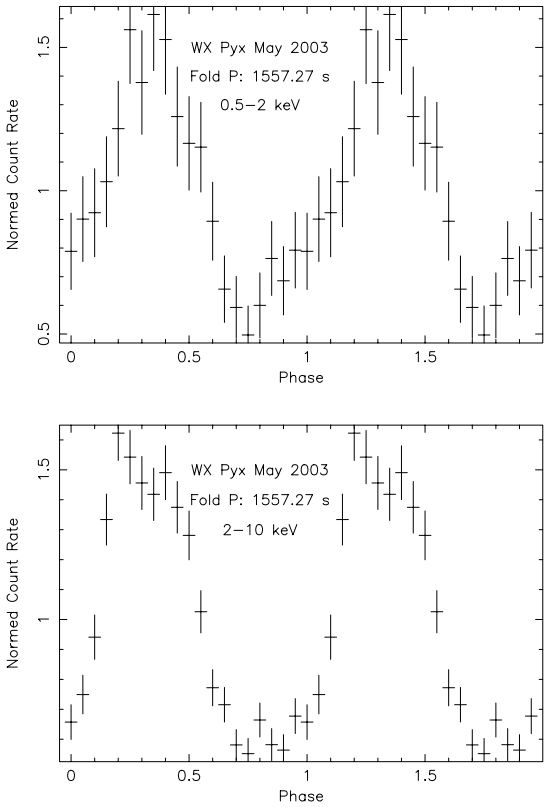

Fig. 3. Normalized X-ray light curves in the (*top*) 0.5–2 and (*bottom*) 2–10 keV bands and folded at the measured spin period. The normalization factors are soft: 0.0459 cts s^{-1} and hard: 0.2013 cts s^{-1}.

one parameter of interest. The modulation period was of the order of 20 ks with large errors owing to the rather few number of points in the orbital curve (∼19), but consistent with the derived candidate orbital period.

Also note that a signal at ∼1230 s (detected frequency = 8.121 ∼ 10^{-4} Hz) is also detected. *XMM-Newton* does not dither owing to the large EPIC pixels, so power at this frequency can not be so attributed. The difference between the detected frequency and the spin frequency is $\sim 1.698 \times 10^{-4}$ and does not correspond to a low-order integer of the spin or orbital periods.

The soft and hard light curves from the May PN data were also folded at the spin period. Figure 3 shows the results. Both bands exhibit sinusoid-like behavior. The origin for each phase fold used the O'Donoghue et al. (1996) definition for phase 0.0. They defined phase 0.0 to be the time of the maximum of the pulse. As the time has drifted by ∼0.35 in phase, the spin period is either known insufficiently accurately or a small change in the period is present. The April PN folded light curve is consistent in shape with the May curve but with considerably less statistical precision.

4. Spectral fit

Energy spectra were extracted using apertures of radius ∼1′.5 centered on the source; from the calibration handbook, an aperture of this size located ∼10′ offaxis will enclose >98% of the events including hard events near 9–10 keV. As the object lies near the chip edges, there is insufficient chip area for a surrounding annulus. The background was obtained from an aperture of identical size positioned south of the source so that no overlap occurred between the source and background apertures. Redistribution matrices and effective areas were built for each spectrum using the SAS version 6.0 routines `rmfgen` and `arfgen`.

A simultaneous fit was carried out on the four extracted spectra: observation-1 PN; observation-2 MOS-1, MOS-2, and PN. Channels less than 0.25 keV and greater than 20.0 keV were ignored in the fit. An absorbed thermal bremsstrahlung and an absorbed power law model were fit to the spectra; both provide reasonably good fits to the continuum. No evidence exists for an iron line, or any line emission; a fit including a zero-width gaussian, to simulate an unresolved line, leads to an upper limit on the presence of Fe line emission of ∼300 eV. Figure 4 shows the final fit to the four spectra. Note that the

Table 2. Simultaneous energy spectrum fits.

					Flux	
Model	χ^2/ν	d.o.f.	$N_{\rm H}$	kT or Γ	0.5–2	2–10
Bremss	0.81	9464	<0.8	18^{+24}_{-6}	4.6	19
Power law	0.60	9464	<0.7	$1.44^{+0.06}_{-0.07}$	4.5	20

Note: $N_{\rm H}$ units = 10^{20} cm^{-2}; unabsorbed fluxes in units of 10^{-13} erg s^{-1} cm^{-2}.

Table 3. Epoch fits to EPIC-PN spectra.

				Brems	Flux	
Month	χ^2/ν	d.o.f.	$N_{\rm H}$	kT	0.5–2	2–10
Apr	0.75	3949	$1.4^{+1.7}_{-1.2}$	<70	0.6	2.6
May	0.82	3949	<0.8	23^{+40}_{-8}	4.4	13

Note: $N_{\rm H}$ units = 10^{20} cm^{-2}; unabsorbed fluxes in units of 10^{-13} erg s^{-1} cm^{-2}.

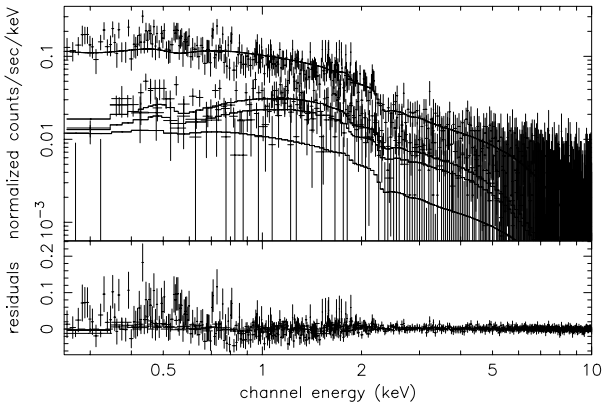

Fig. 4. Simultaneous model fit to the EPIC-PN, -MOS1, -MOS2 spectra from the May observation and the EPIC-PN spectrum from the April observation. No credible evidence exists for any Fe emission, or any other lines. The May PN spectrum is uppermost of the stack; the April PN spectrum lies among the MOS spectra. The model shown does not include a line component, so any line emission should appear in the residuals.

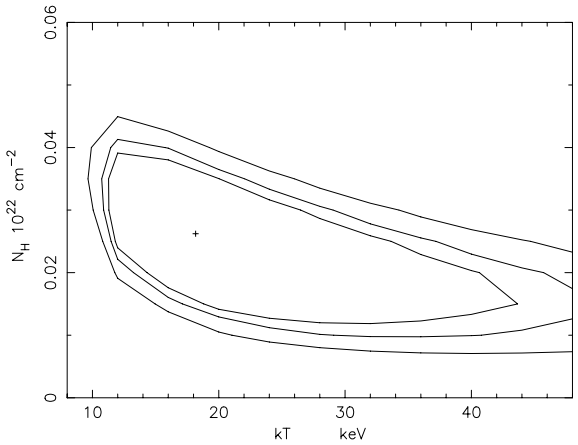

Fig. 5. Contour plot for the bremsstrahlung temperature and column density $N_{\rm H}$. The contours correspond to the 1σ, 90%, and 99% levels in $\Delta\chi^2$ for 2 parameters of interest.

top-most histogram is the May PN spectrum; the Apr PN spectrum lies about a factor of 10 lower. The contour plot for the bremsstrahlung temperature and column density $N_{\rm H}$ is shown in Fig. 5.

The mean fluxes in the 0.5–2 and 2–10 keV bands are $\sim 4.6 \times 10^{-13}$ and $\sim 2.3 \times 10^{-13}$ erg s^{-1} cm^{-2}, as listed in Table 2. The corresponding luminosities are $\sim 5.5 \times 10^{29}$ d^2_{100} and $\sim 2.3 \times 10^{30}$ d^2_{100} erg s^{-1}, respectively, using an adopted distance of 100 d_{100} pc.

Clearly visible is the difference in flux between the Apr. and May PN spectra, a factor of ~10. A fit to the spectra separately shows a temperature broadly consistent between the two epochs (the Apr. observation only yields an upper limit), but the column density differs. The April observation produces a specific $N_{\rm H}$ value, albeit with large error bars because of the low count rate. The May observation leads to an upper limit on the column density.

For each epoch, upper limits may also be assigned to the equivalent widths for potential line emission. Adopting a Gaussian with zero width (to simulate an unresolved line), the 90% upper limits for the April PN spectrum are ~100 eV at 1.7 keV (Si) and ~185 eV at 6.7 keV; the May PN values are ~50 eV (Si) and 390 eV (Fe). The high value in May corresponds to a higher count rate in the hard band; an examination of the events in the 5.5–7.5 keV band shows considerable noise, but no line emission.

5. Discussion

O'Donoghue et al. (1996) found a spin period of 1557.5 ± 0.2 s in optical photometry from 1996. The *XMM* data indicate a spin period of 1557.3 s and set a limit of $\sim 1.5 \times 10^{-6}$ s s^{-1} on a period change over the intervening ~8 years.

The folded optical variation was nearly sine-like in the repeated pulse shapes, but not exactly a sinusoid: the rise toward the peak occurred slowly at first, then more rapidly. This description mimics the soft band *XMM* light curve (modulo the phase shift); if the slope change identified by O'Donoghue et al. at phase ~0.62 exactly matches that in the soft X-ray curve, then the phase shift is ~0.45, larger than but not inconsistent with the ~0.35 shift identified from the locations of the pulse peaks.

The hard band light curve is more steep-sided, as if a hot region that would generate a sinusoid light curve simply through geometric projection, were buried such that the observer needed to be nearly normal to it for it to be visible. Simulated light curves (e.g., Kim & Beuermann 1995) show sinusoidal behavior at high energies and more square-wave behavior at low energies.

The difference in flux by a factor of ~10 in a few weeks is not necessarily surprising given the high-low state behavior of IPs (e.g., GK Per; Hellier et al. 2004). The difference does not appear to be confined to one portion of the spectrum as one might expect if, for example, enhanced accretion led to a higher column density. The flux in both the soft and hard bands changed by similar factors. By way of an explanation, perhaps the *XMM* observation caught WX Pyx emerging from a low state.

The strength of the spin component relative to the $\omega \pm \Omega$ components suggests disk accretion occurs in WX Pyx given the weak orbital modulation (Norton et al. 1996). That supposition must be confirmed, however, with a longer observation as the *XMM* observation only covers roughly 1.5 $P_{\rm orb}$. A weak orbital modulation likely indicates a low inclination, following the results of, for example, Hellier & Mason (1990). The strengths of the sidebands are ~0.3 and 0.2, respectively, for the $\omega - \Omega$ and $\omega + \Omega$ relative to the strength of the spin period. These values are well within the range of behavior observed for disk-overflow IPs such as FO Aqr and imply that a pure disk accretion interpretation is insufficient (Norton et al. 1996). Furthermore, given the factor of ~10 change in observed flux and if WX Pyx was emerging from a low state, then the disk may have been recovering, thereby artificially weakening any spin-orbit-coupled emission. Long-term monitoring observations should be useful to establish any high-low state changes and provide context for the observations described here.

If the estimated orbital period of ~19 933 s is confirmed, then the $P_{\rm spin}/P_{\rm orb}$ ratio is ~0.08, placing WX Pyx in the $P_{\rm spin} - P_{\rm orb}$ plane as a neighbor of the Cols, TV and TX. This is an intriguing trio of objects given their range of observed behavior. WX Pyx shows little iron emission and varies by a factor of ~10 in intensity over ~month times. TV Col displays multiple periodicities and strong Fe emission (Rana et al. 2004). TX Col exhibits considerable variation in power spectra components over times perhaps as short as a day (Schlegel & Salinas 2004; Schlegel 2005). While the magnetic moment-$P_{\rm spin}$ scenario described by Norton et al. (2004) is intellectually unifying, there must be an additional parameter that dictates different behavior from three IPs with nearly identical $P_{\rm spin}/P_{\rm orb}$ ratios.

Acknowledgements. The research of E.M.S. was supported by contract number NAS8-39073 to SAO.

References

Beasley, A. J., Bastian, T. S., Ball, L., & Wu, K. 1994, AJ, 108, 2207
Buckley, D. A. H. 2000, NewAR, 44, 63

Hellier, C., Harmer, S., & Beardmore, A. P. 2004, MNRAS, 349, 710
Hellier, C., & Mason, K. O. 1990, in Accretion Processes in Astrophysics, ed. C. Mauche (Cambridge: Cambridge Univ. Press), 185
Hertz, P., & Grindlay, J. E. 1984, ApJ, 278, 137
Hertz, P., Bailyn, C. D., Grindlay, J. E., et al. 1990, ApJ, 364, 251
Hoard, D. W., Wachter, S., Clark, L. L., & Bowers, T. P. 2002, ApJ, 565, 511
Kazarovets, E. V., Samus, N. N., & Goranskij, V. P. 1993, IBVS 3840
Kim, Y., & Beuermann, K. 1995, A&A, 298, 165
Norton, A. J., Wynn, G. A., & Somerscales, R. V. 2004, ApJ, 614, 349
Norton, A. J., Beardmore, A. P., & Taylor, P. 1996, MNRAS, 280, 937
O'Donoghue, D., Koen, C., & Kilkenny, D. 1996, MNRAS, 278, 1075
Pavelin, P. E., Spencer, R. E., & Davis, R. J. 1994, MNRAS, 269, 779
Rana, V. R., Singh, K. P., Schlegel, E. M., & Barrett, P. 2004, AJ, 127, 489
Schlegel, E. M., & Salinas, A. 2004 in Proc. Cape Town Magnetic CV Workshop, ed. M. Cropper & S. Vrielmann (San Francisco: ASP)
Schlegel, E. M. 2005, in preparation
Szkody, P., Garnavich, P., Howell, S., & Kii, T. 1990, in Accretion-Powered Compact Binaries, ed. C. Mauche (Cambridge: Cambridge Univ. Press), 251
Warner, B. 1995, Cataclysmic Variables (Cambridge: Cambridge Univ. Press)
Wendker, H. J. 1995, A&AS, 109, 177